

Embodiment-Induced Coordination Regimes in Tabular Multi-Agent Q-Learning

Muhammad Ahmed Atif¹ Nehal Naeem Haji¹ Mohammad Shahid Shaikh¹ Muhammad Ebad Atif¹

Abstract

Centralized value learning is often assumed to improve coordination and stability in multi-agent reinforcement learning, yet this assumption is rarely tested under controlled conditions. We directly evaluate it in a fully tabular predator-prey gridworld by comparing independent and centralized Q-learning under explicit embodiment constraints on agent speed and stamina. Across multiple kinematic regimes and asymmetric agent roles, centralized learning fails to provide a consistent advantage and is frequently outperformed by fully independent learning, even under full observability and exact value estimation. Moreover, asymmetric centralized-independent configurations induce persistent coordination breakdowns rather than transient learning instability. By eliminating confounding effects from function approximation and representation learning, our tabular analysis isolates coordination structure as the primary driver of these effects. The results show that increased coordination can become a liability under embodiment constraints, and that the effectiveness of centralized learning is fundamentally regime and role-dependent rather than universal.

1. Introduction

Centralized training is commonly assumed to improve coordination, stability, and performance in multi-agent reinforcement learning. This assumption underlies a broad class of centralized value methods and centralized-training decentralized-execution paradigms, and is often treated as a default design choice rather than an empirical question.

¹Dhanani School of Science and Engineering, Habib University, Karachi, Pakistan. Correspondence to: Muhammad Ahmed Atif <muhammad.atif@habib.edu.pk>, Nehal Naeem Haji <nh07884@st.habib.edu.pk>, Mohammad Shahid Shaikh <shahid.shaikh@sse.habib.edu.pk>, Muhammad Ebad Atif <ma09639@st.habib.edu.pk>.

Preliminary work. Under review by the International Conference on Machine Learning (ICML). Do not distribute.

In embodied multi-agent settings, however, coordination and performance need not align. Constraints on agent speed, stamina, and action timing can couple decisions in ways that reduce strategic flexibility, distort resource allocation, or amplify small coordination errors. Under such conditions, increased coordination may stabilize joint behavior while simultaneously degrading effectiveness.

In this work, we show that centralized coordination is not monotonically beneficial, even in fully observable tabular environments with exact value estimation. Using a controlled predator-prey gridworld with explicit embodiment constraints, we demonstrate that speed and stamina systematically modulate the effectiveness of centralized learning, producing regime-dependent reversals in which decentralized learning outperforms centralized alternatives.

The predator-prey paradigm provides a particularly sharp stress test for coordination assumptions because it combines asymmetric agent roles with tightly coupled interaction dynamics. Predators often benefit from coordinated pursuit and role specialization, whereas prey success depends on decentralized adaptation, evasive behavior, and strategic flexibility. This asymmetry creates regimes in which increased coordination can either support or undermine task performance, depending on how learning structure interacts with embodied constraints.

As a result, predator-prey environments expose a fundamental tension that is often obscured in symmetric cooperative benchmarks. Coordination mechanisms that stabilize learning for one role may simultaneously induce brittleness or reduced adaptability for another. This makes predator-prey a principled setting for interrogating whether centralized learning structures genuinely confer general advantages, rather than reflecting design biases embedded in commonly used benchmarks.

To interrogate coordination assumptions rather than merely compare empirical performance, this study deliberately adopts a tabular formulation. Tabular MARL exposes the full state-action value structure, enabling direct inspection of learning dynamics, coordination failure modes, and policy coupling effects that are typically obscured by function approximation. In this setting, differences between inde-

pendent and centralized learning cannot be attributed to representational capacity or optimization artifacts, but instead arise from coordination structure itself.

Accordingly, we conduct a comparative analysis of four tabular single RL reduction configurations, focusing on Independent Q Learning and Centralized Q Learning variants within a predator prey environment that includes explicit speed and stamina constraints. This study is guided by the following questions:

1. Does centralized value learning reliably improve performance?
2. Can increased coordination degrade effectiveness under embodied constraints?
3. How do coordination structures alter emergent behavior and failure modes across asymmetric roles?
4. Do algorithmic advantages reverse between predator and prey roles?

To address these questions, we perform a controlled empirical study comparing all predator prey algorithm pairings in a fully observable GridWorld while holding environment dynamics and learning rules fixed. Our findings suggest that the benefits of centralized coordination are contingent on embodied factors and agent roles, with regimes in which centralized learning aligns with improved performance as well as regimes in which its advantages diminish or reverse. These results motivate a more nuanced view of coordination in MARL, emphasizing the interaction between learning structure, embodiment, and role asymmetry rather than assuming uniform benefits from increased coordination.

2. Literature Review

Foundational surveys and method-oriented syntheses establish the conceptual scaffolding for this study but leave unresolved a concrete empirical question at the intersection of tabular Independent Q-Learning (IQL), Centralized Q-Learning (CQL), and embodied constraints such as speed and stamina. Canonical treatments of tabular reinforcement learning formalize Q-update rules, convergence properties, and evaluation criteria, providing the theoretical vocabulary required for controlled algorithmic comparison and interpretability (Sutton & Barto, 2018). Broader overviews contextualize algorithm families, exploration strategies, and common failure modes, justifying tabular benchmarks as a methodological laboratory that trades ecological complexity for analytical clarity and reproducibility (Pecioski et al., 2023).

Within multi-agent reinforcement learning (MARL), survey taxonomies position the IQL–CQL trade-off as a central

design axis, highlighting tensions between scalability, non-stationarity, and coordination failure (Panait & Luke, 2005). Subsequent syntheses advocating centralized training with decentralized execution emphasize experimental rigor and baseline construction, even within tabular regimes (Albrecht et al., 2024). Analyses of learning dynamics further show that independent updates can induce instability or slow convergence under heterogeneous incentives and asymmetric roles (Claus & Boutilier, 1998), while evolutionary and dynamical-systems perspectives demonstrate how agent heterogeneity can qualitatively alter learning trajectories and equilibrium selection (Bloembergen et al., 2015). Related work on agent modeling indicates that explicit modeling can improve coordination in pursuit–evasion settings, motivating structured comparisons among independent, modeled, and centralized learners (Albrecht & Stone, 2018). Despite this mature taxonomy, existing surveys do not resolve how tabular IQL and CQL compare empirically in predator–prey environments when agents are subject to explicit, parameterized speed and stamina constraints.

The choice of a tabular setting is therefore methodological rather than pragmatic. By operating in a fully enumerated state–action space, tabular reinforcement learning enables exact inspection of learned value functions and isolates coordination structure from confounding effects introduced by representation learning and optimization. This permits principled attribution of observed performance differences to learning structure rather than auxiliary effects.

Beyond algorithmic structure, designer priors such as reward shaping and initialization are known to exert first-order influence on tabular learning outcomes, accelerating learning while potentially confounding comparisons if not carefully controlled (Rosenfeld et al., 2017). Accordingly, experimental protocols must explicitly isolate coordination effects from engineered priors to preserve internal validity.

Predator–prey environments provide a principled testbed where these methodological concerns intersect with embodied constraints. Empirical and theoretical studies show that pursuit and escape dynamics depend nonlinearly on trade-offs among speed, maneuverability, and energetic limitations, motivating models with explicit stamina costs and heterogeneous action capabilities (Howland, 1974; Wheatley et al., 2015). Such constraints induce asymmetric interaction regimes and strong coupling, conditions under which coordination mechanisms may either stabilize or degrade learning dynamics (Hernandez-Leal et al., 2017).

Despite extensive study of independent and centralized learning, prior work does not isolate how coordination structure interacts with explicit embodiment constraints under controlled tabular conditions. Existing studies typically confound coordination effects with representation learning, optimization dynamics, or symmetric cooperative objectives.

As a result, it remains unclear whether reported advantages of centralization arise from coordination structure itself or from auxiliary effects introduced by function approximation. This study directly addresses this gap by isolating coordination mechanisms in a fully enumerated state-action space.

3. Background and Overview

Reinforcement learning (RL) enables agents to learn optimal behaviors through trial-and-error interactions with their environment, guided by reward signals. The standard formulation is the Markov Decision Process (Sutton & Barto, 2018).

The core objective is to learn the optimal action-value function $Q^*(s, a)$, which estimates the expected cumulative future reward. The Bellman equation provides the recursive relationship:

$$Q^*(s, a) = \mathbb{E}_{s'} \left[R(s, a) + \gamma \max_{a'} Q^*(s', a') \right] \quad (1)$$

Q-learning solves this via iterative value updates without requiring knowledge of the environment dynamics (model-free):

$$Q(s, a) \leftarrow Q(s, a) + \alpha \left[r + \gamma \max_{a'} Q(s', a') - Q(s, a) \right] \quad (2)$$

where α is the learning rate. Under standard conditions, tabular Q-learning converges to Q^* with probability 1 (Watkins & Dayan, 1992).

3.1. Game-Theoretic Models for Multi-Agent Interaction

When multiple agents interact in a shared environment, the MDP formalism must be extended to account for the strategic interactions between agents. Multi-agent reinforcement learning (MARL) employs a hierarchy of game-theoretic models that progressively add structure and realism.

3.1.1. STOCHASTIC GAMES

We model the predator-prey environment as a stochastic game, a multi-agent extension of the Markov Decision Process in which agents interact through a shared state and joint actions. At each timestep, agents select actions based on the current state, receive role-specific rewards, and transition to a new state according to the environment dynamics. This formulation naturally captures pursuit-evasion interactions with embodied attributes such as position, speed, and stamina.

3.2. Single-Agent RL Reductions in Multi-Agent Settings

Multi-agent reinforcement learning (MARL) extends RL to settings with N agents simultaneously learning and interacting. A Multi-Agent MDP (MM-MDP) defines the joint state space S , joint action space $\mathbf{A} = A_1 \times \dots \times A_N$, and joint reward function $\mathbf{R}(s, \mathbf{a}) = (r_1, \dots, r_N)$. Each agent i learns a policy $\pi_i : O_i \rightarrow A_i$ to maximize its expected cumulative reward $J_i = \mathbb{E}[\sum_t \gamma^t r_i(s_t, \mathbf{a}_t)]$ (Busoniu et al., 2008).

The simplest approach to MARL is to reduce the multi-agent problem to single-agent learning problems, either by centralizing control (Central Q-Learning) or by treating other agents as part of the environment (Independent Q-Learning) (Albrecht et al., 2024).

3.3. Independent Q-Learning (IQL)

In IQL, each agent i independently maintains and updates its own Q-function $Q_i(s_i, a_i)$ using Eq. 2, treating other agents as part of the environment. This avoids the scalability issue of joint spaces but suffers from non-stationarity and poor credit assignment due to local, individual rewards (Albrecht et al., 2024). Full pseudocode is provided in Appendix C.

3.4. Centralized Q-Learning (CQL)

CQL maintains a single centralized Q-function $Q_{\text{total}}(s, \mathbf{a})$ that evaluates joint actions (a_1, \dots, a_N) using access to the full global state s and summed rewards $r_{\text{total}} = \sum_i r_i$ during training. This eliminates non-stationarity and improves credit assignment but introduces policy extraction complexity at execution time (Albrecht et al., 2024). Full pseudocode is provided in Appendix C.

Key Trade-off: IQL is simple and scalable but suffers from non-stationarity and poor credit assignment. CQL improves learning stability and credit assignment through centralized training but faces exponential scalability in the joint action space and requires policy extraction for decentralized execution. This paper empirically compares IQL and CQL in a predator-prey environment with explicit speed and stamina constraints to identify conditions under which centralization provides measurable benefits.

4. Experimental Setup

4.1. Environment and State Representation

We evaluate tabular Independent Q-Learning (IQL) and Centralized Q-Learning (CQL) in a discrete, fully observable multi-agent environment on an 8×8 grid. The environment encodes global state as positions and internal attributes (stamina, speed and team). Both Independent Q-

Learning and Centralized Q-Learning use the full joint state for value estimation. Local observations are used only to define decentralized execution interfaces and do not restrict the information available to the value functions (Anonymous, 2025).

4.2. Action Model and Embodiment Constraints

Agents execute discrete actions from $\mathcal{A} = \{\text{UP, DOWN, LEFT, RIGHT, STAY}\}$. We implement a micro-stepping mechanism where agent i with speed v_i executes up to v_i moves per timestep. Collision detection prevents agents from occupying the same cell or moving into obstacles. A stamina system depletes per move, constraining resources.

Rewards make use of potential-based shaping. Predators receive a capture reward of +100 when occupying the same cell as a prey, along with a per-step penalty of -5. Prey agents receive no intermediate rewards and incur a terminal penalty of -100 upon capture. Potential-based shaping is applied using a distance-based potential

$$\Phi_i(s) = \sum_j w_i d_{ij}(s), \quad (3)$$

encouraging predators to minimize and prey to maximize distance to the nearest opposing agents. Shaping rewards are computed as:

$$F(s, s') = \gamma \Phi(s') - \Phi(s), \quad (4)$$

which preserves the optimal policy under standard assumptions (Devlin & Kudenko, 2012; Ng et al., 1999). Because identical potential-based shaping is applied across all learning configurations, any shaping-induced bias affects all conditions symmetrically and does not explain the observed relative performance differences.

Episodes terminate upon capture of all prey or reaching a maximum of 200 timesteps.

4.3. Learning Algorithms

Independent Q-Learning (IQL): We deliberately allow IQL agents access to the full joint state to isolate coordination effects from partial observability, making our IQL a decentralized-action, centralized-state baseline. That is, each agent i independently maintains a Q-function $Q^i(s, a_i)$, updating via standard tabular Q-learning where $\alpha = 0.25$ and $\gamma = 0.90$ (see Appendix A). IQL treats other agents as part of the environment, which induces non-stationarity and can hinder credit assignment and coordination.

Centralized Q-Learning (CQL): A centralized learner maintains $Q^{\text{total}}(s, a)$ evaluating joint actions where $r_{\text{total}} = \sum_i r_i$ and $\alpha = 0.25$, $\gamma = 0.90$ (see Appendix A). Decentralized execution uses marginalization: $Q^{\text{marg}}(s, a_i) =$

$\mathbb{E}_{\mathbf{a}_{-i}}[Q^{\text{total}}(s, a_i, \mathbf{a}_{-i})]$, with each agent executing $a_i^* = \arg \max_{a_i} Q^{\text{marg}}(s, a_i)$. During execution, agents condition only on their own action component derived from the joint-state value. Our CQL corresponds to classical joint-action tabular learners, not modern CTDE deep methods. This choice is deliberate: scalability is traded for exact coordination structure isolation.

The tabular setting is a deliberate methodological choice rather than a limitation. By eliminating confounding effects introduced by function approximation, partial observability, and representation learning, the experimental design ensures that observed performance differences arise solely from coordination structure and embodiment constraints. In this regime, centralized and independent learners differ only in how they couple actions and assign credit, enabling direct attribution of observed effects.

4.4. Experimental Conditions

The experiments are designed to quantify how algorithmic configuration and embodied kinematic constraints jointly influence learning dynamics and performance in a tabular predator-prey multi-agent environment. We focus on contrasting Independent Q-Learning (IQL) and Centralized Q-Learning (CQL) under controlled conditions to isolate the effects of coordination structure and agent embodiment. Since both Independent Q-Learning and Centralized Q-Learning operate over the same full joint state representation, observed performance differences can be attributed to differences in action coupling and credit assignment rather than differences in information availability.

We evaluate four learning configurations obtained by assigning either IQL or CQL to each agent role: IQL-IQL, IQL-CQL, CQL-IQL, and CQL-CQL, where the first term denotes the predator learning paradigm and the second denotes the prey paradigm. Each configuration is evaluated under three distinct speed regimes, yielding a total of twelve experimental conditions.

Speed is treated as a discrete experimental factor with two operational modes: base speed, in which an agent moves one grid cell per timestep at a cost of one stamina unit, and double speed, in which an agent moves two grid cells per timestep at a cost of two stamina units. The three speed regimes considered are:

1. equal base speed for predators and prey,
2. double speed for predators only, and
3. double speed for prey only.

A regime in which both predators and prey have double speed is excluded, as it is functionally equivalent to a scaled version of the equal-speed setting under the fixed stamina

budget and introduces unnecessary variance without providing additional insight.

4.5. Training Protocol

All configurations are trained for 40,000 episodes. Experiments are repeated over 10 independent random seeds, with identical seeds reused across configurations to enable paired statistical comparisons. Apart from the manipulated factors (learning configuration and speed regime), all aspects of the environment and learning setup, including reward shaping, learning rates, discount factors, and the exploration policy, are held constant across conditions. Action selection follows an ϵ -greedy policy with ϵ exponentially decayed from 1.0 to 0.1 over the first 23,000 episodes and held constant thereafter.

4.6. Evaluation Metrics

Performance is evaluated using episode length, predator reward and prey reward. Episode length and predator reward reflect coordination efficiency and pursuit effectiveness, while prey reward captures survival dynamics under different learning configurations. Final performance metrics are computed by averaging over the last 10,000 training episodes, during which learning curves empirically stabilize across all configurations.

Performance is evaluated using the following metrics:

- **Episode Length:** Average timesteps until termination (capture or timeout).
- **Mean Predator Reward:** Average cumulative reward obtained by predator team per episode.
- **Mean Prey Reward:** Average cumulative reward obtained by prey team per episode.

All metrics are computed at the seed level by averaging over the final 10,000 training episodes, during which learning curves empirically stabilize.

4.7. Statistical Analysis

All statistical analyses are conducted on seed-level performance summaries rather than episode-level data since episode-level data is not independent and identically distributed (Billingsley, 2012). For each seed, metrics are computed as means over the final 10,000 episodes. Pairwise comparisons are performed using the Wilcoxon signed-rank test (Wilcoxon, 1945), with effect sizes reported via Cliff’s delta (Cliff, 1993). Holm–Bonferroni correction (Holm, 1979) is applied to account for multiple comparisons. Corrections are applied separately within each speed regime across all pairwise comparisons of learning configurations for a given evaluation metric.

5. Results

We evaluate Independent Q-Learning (IQL) and Centralized Q-Learning (CQL) across three kinematic regimes and four role-specific learning configurations in order to isolate how coordination structure interacts with embodiment constraints. Rather than treating centralization as uniformly beneficial, our analysis focuses on identifying regime-level patterns in which learning structure either stabilizes coordination or induces systematic failure. All reported metrics are computed as seed-level averages over the final 10,000 training episodes across 10 independent random seeds, and statistical comparisons are conducted using paired non-parametric tests with correction for multiple comparisons.

Our analysis focuses not on identifying a single best-performing algorithm, but on characterizing regime-dependent coordination behavior. Results are therefore interpreted in terms of systematic reversals and failure modes induced by learning structure and embodiment constraints, rather than absolute performance rankings. This perspective reveals patterns that would be obscured by aggregate comparisons.

5.1. Base Speed Regime

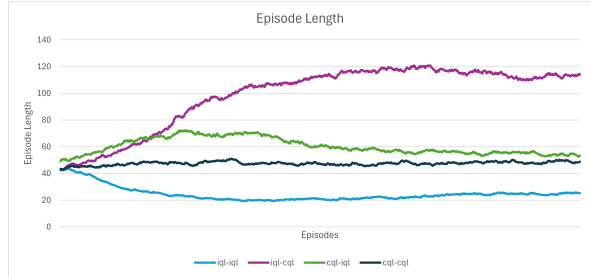


Figure 1. Mean episode length over training under the base-speed regime. Curves show the mean across 10 independent seeds. Lower values correspond to more efficient predator coordination.

Under the base-speed regime, where predators and prey possess equal mobility and identical stamina constraints, performance differences arise solely from learning structure rather than kinematic asymmetry. As shown in Figure 1, learning curves diverge early and stabilize into distinct regimes. Fully independent learning (IQL–IQL) consistently converges to the shortest episodes, indicating more efficient pursuit and capture dynamics, while mixed configurations—particularly IQL–CQL—exhibit substantially longer episodes and higher variance.

Seed-level statistical analysis confirms these trends (see Section V-D): IQL–IQL achieves significantly shorter episodes and higher predator rewards than CQL–CQL (paired Wilcoxon signed-rank test, $p = 0.00195$, Cliff’s $\delta = 1.0$).

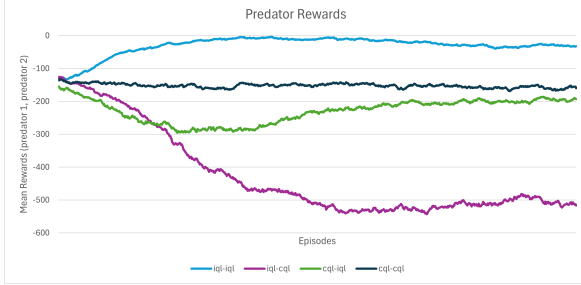


Figure 2. Mean predator reward over training under the base-speed regime. Curves show the mean across 10 independent seeds. Higher values correspond to faster and more efficient capture behavior.

Predator reward trajectories (Figure 2) mirror the episode-length results. IQL–IQL attains the highest final predator returns, while IQL–CQL performs worst, indicating that asymmetric learning structures degrade credit assignment and disrupt coordinated pursuit even in symmetric environments.

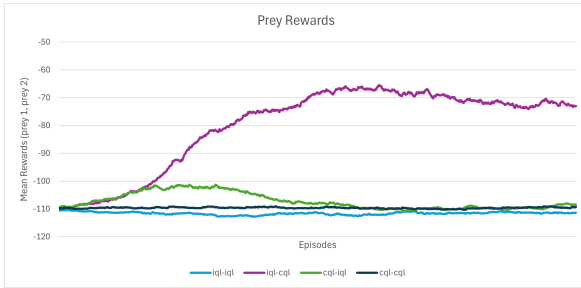


Figure 3. Mean prey reward over training under the base-speed regime. Curves show the mean across 10 independent seeds. Higher rewards correspond to longer survival times.

Prey rewards exhibit the inverse pattern: configurations that induce efficient predator coordination, especially IQL–IQL, result in lower prey returns due to faster capture, whereas prey benefit most under mismatched learning structures that prolong episodes. Together, these results show that under equal-speed conditions, learning-structure alignment dominates performance, and increased centralization does not guarantee improved coordination.

5.2. Predator Speed Advantage

When predators possess a speed advantage, coordination demands intensify and performance gaps between learning configurations widen. As shown in Figure 4, IQL–IQL converges rapidly to very short episodes, indicating effective exploitation of increased mobility. In contrast, centralized and mixed configurations exhibit longer episodes and slower convergence, suggesting difficulty translating kinematic advantage into coordinated capture.

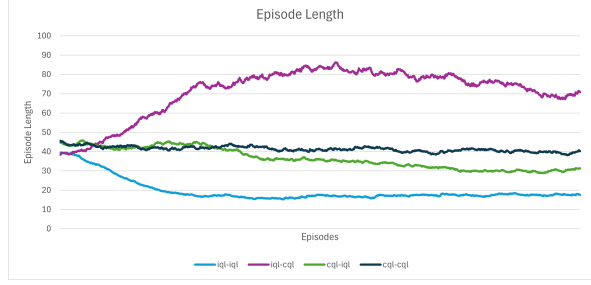


Figure 4. Mean episode length over training under the predator-speed-advantage regime. Curves show the mean across 10 independent seeds. Lower values correspond to more efficient predator coordination.

Under predator speed advantage, configuration effects are amplified, with IQL–IQL significantly outperforming CQL–CQL in both episode length and predator reward across all seeds (paired Wilcoxon signed-rank test, $p = 0.00195$, Cliff’s $\delta = 1.0$; see Section V-D).

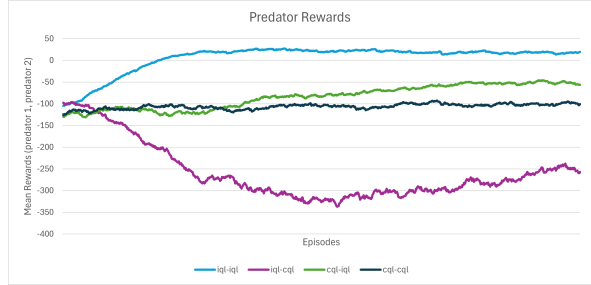


Figure 5. Mean predator reward over training under the predator-speed-advantage regime. Curves show the mean across 10 independent seeds. Higher rewards reflect improved exploitation of kinematic advantage through coordination.

From the prey perspective, decentralized predator learning induces the lowest survival rewards, reflecting rapid capture. Mixed configurations, particularly IQL–CQL, substantially prolong episodes and increase prey rewards, indicating that learning-structure mismatch overwhelms the benefits of predator speed advantage. This regime demonstrates that increased mobility amplifies the consequences of learning-structure alignment rather than uniformly favoring centralized coordination.

5.3. Prey Speed Advantage

Under prey speed advantage, overall episode lengths increase across all configurations, reflecting enhanced evasion capability and reduced capture efficiency. As shown in Figure 6, learning curves cluster more closely than in previous regimes, indicating a partial narrowing of performance gaps. Nonetheless, systematic differences persist: configurations that disrupt predator coordination produce the longest episodes, while fully independent predator learning remains

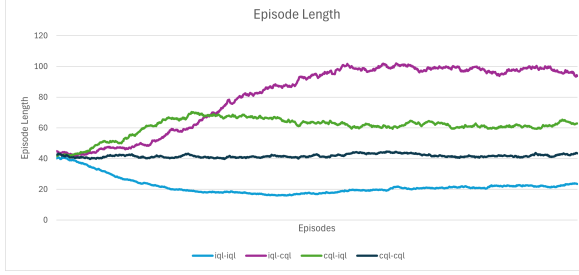


Figure 6. Mean episode length over training under the prey-speed-advantage regime. Curves show the mean across 10 independent seeds. Higher values indicate increased prey survival due to enhanced evasion capability.

comparatively robust.

When prey possess a speed advantage, statistically significant differences persist but effect sizes narrow, with IQL–IQL continuing to yield shorter episodes and higher predator rewards than CQL–CQL (paired Wilcoxon signed-rank test, $p = 0.00195$, Cliff’s $\delta = 1.0$; see Section V-D).

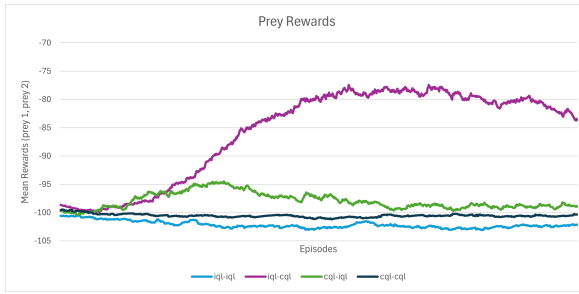


Figure 7. Mean prey reward over training under the prey-speed-advantage regime. Curves show the mean across 10 independent seeds. Higher rewards indicate improved evasion and prolonged survival.

In this regime, prey rewards are highest under configurations that induce predator coordination failure, particularly IQL–CQL, while fully independent predator learning suppresses prey survival most effectively. These results indicate that increased prey mobility attenuates but does not eliminate the influence of learning structure, and that centralization provides diminishing returns when evasion dominates interaction dynamics.

In several metrics, decentralized prey learning matches or exceeds centralized alternatives, indicating that centralization provides diminishing returns when prey mobility dominates the interaction dynamics.

Across regimes, the relative advantage of centralized learning is strongly modulated by kinematic constraints. Centralization yields its strongest relative improvements over mismatched configurations when predator coordination pressure is high, while decentralized learning remains competitive when prey speed dominates. These results highlight an

interaction between embodiment and coordination structure that is not captured by algorithm choice alone.

5.4. Statistical Analysis

We next assess whether the performance differences identified in the descriptive results persist reliably across random seeds. To this end, we conduct statistical comparisons on seed-level performance summaries using paired non-parametric tests. Our analysis focuses on theory-motivated contrasts that capture differences in learning configuration and agent role, rather than exhaustive pairwise testing across all conditions.

Under equal-speed conditions, statistically significant differences persist across learning configurations for all metrics. IQL–IQL yields consistently shorter episodes and higher predator rewards than CQL–CQL (Wilcoxon signed-rank test, $p = 0.00195$; Cliff’s $\delta = 1.0$), indicating more efficient pursuit under decentralized learning. Mixed configurations show the strongest divergence: IQL–CQL produces substantially longer episodes and lower predator rewards than CQL–IQL, while simultaneously yielding higher prey rewards ($p \leq 0.00391$; $|\delta| \geq 0.8$). These results demonstrate that coordination structure alone, even without speed asymmetry, strongly shapes emergent performance.

When predators have a speed advantage, configuration effects are amplified. IQL–IQL again achieves significantly shorter episodes and higher predator rewards than CQL–CQL across all seeds ($p = 0.00195$; $\delta = 1.0$), suggesting that independent predators exploit increased mobility most effectively. Mixed configurations exhibit severe coordination failure: IQL–CQL leads to prolonged episodes, reduced predator rewards, and increased prey rewards relative to CQL–IQL ($p = 0.00195$; $\delta = 1.0$). Thus, learning asymmetry dominates even when kinematic conditions favor predators.

Under prey-speed advantage, configuration-dependent effects remain robust. IQL–IQL continues to yield shorter episodes and higher predator rewards than CQL–CQL ($p = 0.00195$; $\delta = 1.0$), indicating greater adaptability of decentralized predators to fast prey. Mixed configurations again produce the largest disparities: IQL–CQL dramatically prolongs episodes and increases prey rewards compared to CQL–IQL, while substantially degrading predator performance ($p = 0.00195$; $\delta = 1.0$). These findings confirm that mismatched learning structures induce persistent coordination breakdowns regardless of which agent class holds a speed advantage.

Across speed regimes, predator performance is maximized under role-aligned learning structures, particularly fully independent learning when predators possess sufficient adaptability or kinematic advantage. In contrast, prey perfor-

mance improves under configurations that induce coordination mismatches among predators, most notably when predator learning is decentralized and prey learning is centralized. Due to Effect sizes frequently saturating due to near-deterministic ordering of configurations across seeds, rather than high variance, the aforementioned patterns are reflected in uniformly large effect sizes, highlighting strong role-dependent sensitivity to learning structure rather than a universal benefit of centralization.

6. Conclusion

This work demonstrates that coordination advantages in multi-agent reinforcement learning are fundamentally contingent on embodiment constraints and agent roles. Through controlled tabular experiments, we show that centralized value learning does not provide a universal benefit and can systematically degrade performance when coordination pressure interacts unfavorably with speed and stamina constraints.

First, we show that tabular single-agent RL reductions are sufficient to induce distinct and stable learning dynamics in multi-agent predator-prey environments, addressing our first research question. Performance differences are not incidental: episode length, predator reward, and prey reward exhibit consistent and interpretable ordering across configurations and seeds.

Second, we find that learning configuration plays a decisive role. Fully role-aligned configurations, particularly IQL-IQL, consistently outperform mixed centralized-independent pairings, while mismatched configurations induce persistent coordination failures. This directly answers our second research question and highlights the risks of asymmetric learning structures in otherwise symmetric environments.

Third, speed and stamina constraints substantially modulate these effects. Predator speed advantage amplifies the benefits of decentralized learning for predators, while prey speed advantage exacerbates coordination breakdowns under mixed configurations. These findings confirm that embodiment constraints are not merely environmental details but actively interact with learning dynamics, addressing our third research question.

Finally, our results clarify which learning paradigms are better suited to different agent roles. Predators benefit most from decentralized learning that enables rapid adaptation, whereas prey benefit from configurations that disrupt predator coordination. This role-dependent sensitivity answers our fourth research question and underscores that no single learning paradigm is universally optimal across roles.

These findings caution against treating centralized coordi-

nation as a default design choice in multi-agent systems. Even under full observability and exact value estimation, increased coordination can induce brittleness, suppress adaptability, and amplify failure modes. By isolating these effects in a controlled tabular setting, this work provides a foundation for principled investigation of coordination mechanisms in more complex embodied and function-approximation-based systems.

7. Impact Statement

This work provides methodological insight into coordination in multi-agent reinforcement learning under embodiment constraints. It is foundational and empirical in scope, with no direct deployment or immediate real-world application, and no anticipated significant societal or ethical impacts.

8. Limitations and Future Work

This study is intentionally restricted to a tabular, fully observable predator-prey environment with a small number of agents. While this design enables controlled experimentation and clear attribution of causal effects, it limits direct generalization to large-scale or function-approximation-based multi-agent systems.

In particular, we do not consider partial observability, communication, or deep function approximation, all of which may alter coordination dynamics and the relative advantages of centralized versus independent learning. Additionally, stamina and speed are modeled in a simplified manner, and more realistic embodiment constraints may introduce further interactions.

Future work should extend this analysis to game-theoretic multi-agent reinforcement learning settings such JAL-GT (Zhang et al., 2021), investigate how these effects scale with agent population size, and examine whether similar coordination pathologies arise under learned representations and partial observability. Another promising direction is to integrate causal or interpretability-focused analysis to better explain why specific learning structures succeed or fail under different embodiment regimes.

References

Albrecht, S. V. and Stone, P. Autonomous agents modelling other agents: A comprehensive survey and open problems. *Artificial Intelligence (AIJ) / CoRR (arXiv preprint)*, 2018. URL <https://arxiv.org/abs/1709.08071>.

Albrecht, S. V., Christianos, F., and Schäfer, L. *Multi-Agent Reinforcement Learning: Foundations and Modern Approaches*. MIT Press, 2024. URL <https://www.marl-book.com>.

Anonymous. Predator-prey archetype gridworld environment, 2025. A discrete testbed for studying Multi-Agent Reinforcement Learning dynamics.

Billingsley, P. *Probability and Measure*. John Wiley & Sons, Hoboken, NJ, 3rd edition, 2012.

Bloembergen, D., Tuyls, K., Hennes, D., and Kaisers, M. Evolutionary dynamics of multi-agent learning: A survey. *Journal of Artificial Intelligence Research (JAIR)*, 2015. URL <https://jair.org/index.php/jair/article/view/10952>.

Busoniu, L., Babuska, R., and De Schutter, B. A comprehensive survey of multiagent reinforcement learning. *Systems, Man, and Cybernetics, Part C: Applications and Reviews, IEEE Transactions on*, 38:156 – 172, 04 2008. doi: 10.1109/TSMCC.2007.913919.

Claus, C. and Boutilier, C. The dynamics of reinforcement learning in cooperative multiagent systems. In *Proceedings of the 15th National Conference on Artificial Intelligence (AAAI-98)*, 1998. URL <https://cdn.aaai.org/AAAI/1998/AAAI98-106.pdf>.

Cliff, N. Dominance statistics: Ordinal analyses to answer ordinal questions. *Psychological Bulletin*, 114(3):494–509, 1993. doi: 10.1037/0033-2909.114.3.494.

Devlin, S. and Kudenko, D. Dynamic potential-based reward shaping. In *Proceedings of the 11th International Conference on Autonomous Agents and Multiagent Systems (AAMAS 2012)*, volume 1, pp. 433–440. International Foundation for Autonomous Agents and Multiagent Systems, 2012.

Hernandez-Leal, P., Kaisers, M., Baarslag, T., and noz de Cote, E. M. A survey of learning in multiagent environments: Dealing with non-stationarity. *CoRR (arXiv)*, abs/1707.09183, 2017. URL <https://arxiv.org/abs/1707.09183>.

Holm, S. A simple sequentially rejective multiple test procedure. *Scandinavian Journal of Statistics*, 6(2):65–70, 1979.

Howland, H. C. Optimal strategies for predator avoidance: the relative importance of speed and manoeuvrability. *Journal of Theoretical Biology*, 47(2):333–350, 1974. doi: 10.1016/0022-5193(74)90202-1. URL [https://doi.org/10.1016/0022-5193\(74\)90202-1](https://doi.org/10.1016/0022-5193(74)90202-1).

Ng, A. Y., Harada, D., and Russell, S. J. Policy invariance under reward transformations: Theory and application to reward shaping. In *Proceedings of the Sixteenth International Conference on Machine Learning, ICML '99*, pp. 278–287, San Francisco, CA, USA, 1999. Morgan Kaufmann Publishers Inc. ISBN 1558606122.

Panait, L. and Luke, S. Cooperative multi-agent learning: The state of the art. *Autonomous Agents and Multi-Agent Systems*, 11(3):387–434, 2005. URL <https://cs.gmu.edu/~eclab/papers/panait05cooperative.pdf>.

Pecioski, D., Gavriloski, V., Markovska, S. D., and Ignjatovska, A. An overview of reinforcement learning techniques. In *Proceedings of the 12th Mediterranean Conference on Embedded Computing (MECO 2023)*, 2023. URL <https://dblp.org>. Conference paper / overview (MECO 2023).

Rosenfeld, A., Cohen, M., Taylor, M. E., and Kraus, S. Leveraging human knowledge in tabular reinforcement learning: A study of human subjects. In *Proceedings of the Twenty-Sixth International Joint Conference on Artificial Intelligence (IJCAI-17)*, pp. 3823–3830, 2017. doi: 10.24963/ijcai.2017/534. URL <https://doi.org/10.24963/ijcai.2017/534>.

Sutton, R. S. and Barto, A. G. *Reinforcement Learning: An Introduction*. MIT Press, 2nd edition, 2018. URL <https://incompleteideas.net/book/the-book-2nd.html>.

Watkins, C. J. C. H. and Dayan, P. Q-learning. *Machine Learning*, 8(3):279–292, 1992. doi: 10.1007/BF00992698. URL <https://doi.org/10.1007/BF00992698>.

Wheatley, R., Jr., M. J. A., and coauthors. How fast should an animal run when escaping? an optimality model based on the trade-off between speed and accuracy. *Integrative and Comparative Biology*, 55(6):1166–1175, 2015. URL <https://academic.oup.com/icb/article/55/6/1166/2363838>.

Wilcoxon, F. Individual comparisons by ranking methods. *Biometrics Bulletin*, 1(6):80–83, 1945.

Zhang, K., Yang, Z., and Basar, T. Multi-agent reinforcement learning: A selective overview of theories and algorithms. *Handbook of Reinforcement Learning and Control*, pp. 321–384, 2021. doi: 10.1007/978-3-030-60990-0_12.

A. Parameters and control settings

Table 1. Parameters and control settings

PARAMETER	DESCRIPTION	VALUE
NUMBER OF PREY AGENTS	COUNT OF INDEPENDENT PREY AGENTS PRESENT IN THE ENVIRONMENT. EACH PREY FOLLOWS THE ASSIGNED ALGORITHMIC CONFIGURATION FOR THE RUN.	2
NUMBER OF PREDATOR AGENTS	COUNT OF PREDATORS. EACH PREDATOR FOLLOWS THE ASSIGNED ALGORITHMIC CONFIGURATION FOR THE RUN.	2
GRID SIZE	DISCRETE GRID WORLD DIMENSIONS (ROWS \times COLUMNS) USED FOR ALL EXPERIMENTS.	8 \times 8
STAMINA (FIXED)	PER-EPSISODE STAMINA BUDGET FOR EACH AGENT. STAMINA IS DEPLETED BY MOVEMENT ACCORDING TO SPEED MODE AND IS A LIMITING RESOURCE TO INDUCE STRATEGIC TRADEOFFS.	5 UNITS
SPEED MODES	BASE SPEED: AGENT MOVES ONE CELL PER ACTION AND EXPENDS 1 STAMINA POINT. DOUBLE SPEED: AGENT MOVES TWO CELLS PER ACTION AND EXPENDS 2 STAMINA POINTS. EXPERIMENTS COMBINE THESE MODES ACROSS AGENT TYPES ACCORDING TO THE THREE SPEED REGIMES DESCRIBED ABOVE.	BASE SPEED, DOUBLE SPEED
ALGORITHMIC PERMUTATIONS	ALL FOUR PAIRINGS OF LEARNING ALGORITHM ASSIGNED TO THE PREDATOR AND PREY AGENT TYPES: (IQL PREDATORS, IQL PREY), (IQL PREDATORS, CQL PREY), (CQL PREDATORS, IQL PREY), (CQL PREDATORS, CQL PREY). EACH PERMUTATION IS EVALUATED UNDER EACH SPEED REGIME.	IQL / CQL COMBINATIONS (4)
DISCOUNT FACTOR (γ)	STANDARD TEMPORAL DISCOUNT FACTOR FOR FUTURE REWARDS USED IN Q-UPDATES.	0.90
LEARNING RATE (α)	STEP SIZE USED IN Q-VALUE UPDATES (ALSO REFERRED TO AS LR).	0.25
RANDOM SEEDS	10 INDEPENDENT SEEDS, SHARED ACROSS CONFIGURATIONS FOR PAIRED COMPARISONS	10
TRAINING DURATION	NUMBER OF TRAINING EPISODES FOR EACH EXPERIMENTAL RUN. PERFORMANCE STATISTICS ARE COMPUTED AFTER TRAINING AND ALSO TRACKED DURING TRAINING FOR LEARNING CURVES.	40,000 EPISODES
EPSILON (EXPLORATION) START	INITIAL VALUE OF ϵ FOR ϵ -GREEDY EXPLORATION.	1.0
EPSILON END	FINAL ϵ AFTER DECAY.	0.1
EPSILON DECAY RATE	THIS PRODUCES A GRADUAL REDUCTION IN EXPLORATION OVER TRAINING.	0.99
DISTANCE PBRs FACTOR	SCALING COEFFICIENT FOR DISTANCE-BASED POTENTIAL-BASED REWARD SHAPING (PBRs). A VALUE OF 1.0 MEANS THE SHAPED POTENTIAL IS APPLIED WITHOUT ADDITIONAL SCALING; THE SHAPING TERM ENCOURAGES AGENTS TO REDUCE (OR INCREASE, DEPENDING ON SIGN) DISTANCE TO TARGET ACCORDING TO THE IMPLEMENTED POTENTIAL FUNCTION.	1.0
PREDATOR CAPTURE PENALTY (BASE REWARD)	TERMINAL OR EVENT REWARD AWARDED TO A PREDATOR UPON SUCCESSFUL CAPTURE OF A PREY AGENT.	+100
PREY CAPTURE PENALTY (BASE REWARD)	PENALTY APPLIED TO PREY AGENTS UPON CAPTURE. PREY RECEIVE NO INTERMEDIATE REWARDS.	-100
PREDATOR STEP COST (BASE REWARD)	PER-STEP PENALTY CHARGED TO PREDATOR AGENTS TO DISCOURAGE UNNECESSARY MOVEMENT AND ENCOURAGE EFFICIENT PURSUIT. THIS IS APPLIED TO PREDATOR REWARD AT EACH TIME STEP.	-5

B. Descriptive Statistics

Table 2. Final performance under the base speed regime, averaged over the last 10,000 episodes and 10 random seeds (mean \pm SD).

CONFIGURATION	EPISODE LENGTH	PREDATOR REWARD	PREY REWARD
IQL-IQL	24.9 ± 9.5	-32.0 ± 44.0	-111.3 ± 3.6
IQL-CQL	113.2 ± 26.4	-505.2 ± 134.3	-72.6 ± 13.5
CQL-IQL	54.4 ± 16.3	-196.1 ± 79.0	-109.1 ± 5.2
CQL-CQL	48.6 ± 14.0	-159.3 ± 69.8	-109.5 ± 3.2

Table 3. Final performance of predator fast speed regime, averaged over the last 10,000 episodes and 10 seeds (mean \pm std)

CONFIGURATION	EPISODE LENGTH	PREDATOR REWARD	PREY REWARD
IQL-IQL	17.5 ± 6.4	18.7 ± 31.2	-101.9 ± 3.1
IQL-CQL	71.4 ± 21.9	-260.1 ± 113.1	-92.0 ± 7.6
CQL-IQL	30.1 ± 8.4	-52.2 ± 40.0	-102.7 ± 3.7
CQL-CQL	40.2 ± 10.6	-101.4 ± 50.7	-100.5 ± 1.7

Table 4. Final performance of prey fast speed regime, averaged over the last 10,000 episodes and 10 seeds (mean \pm std)

CONFIGURATION	EPISODE LENGTH	PREDATOR REWARD	PREY REWARD
IQL-IQL	22.4 ± 9.3	-9.9 ± 39.7	-102.4 ± 3.3
IQL-CQL	96.4 ± 25.1	-400.1 ± 118.1	-81.6 ± 9.6
CQL-IQL	61.5 ± 17.4	-214.1 ± 83.7	-98.9 ± 5.6
CQL-CQL	42.2 ± 11.6	-109.8 ± 51.5	-100.5 ± 2.5

C. Algorithmic Details

Algorithm 1 Independent Q-Learning for Agent i with Potential Based Reward Shaping (Albrecht et al., 2024)

```

1: Initialize:  $Q_i(s, a_i) \leftarrow 0$  for all  $s \in S, a_i \in A_i$ 
2: Repeat for every episode:
3: for  $t = 0, 1, 2, \dots$  do
4:   Observe current state  $s^t$ 
5:   With probability  $\epsilon$ , choose random action  $a_i^t \in A_i$ 
6:   Otherwise, choose  $a_i^t \in \arg \max_{a_i} Q_i(s^t, a_i)$ 
7:   Meanwhile, other agents  $j \neq i$  choose their actions  $a_j^t$ 
8:   Observe own reward  $r_i^t$  and next state  $s^{t+1}$ 
9:    $r'_i(s_i^t, a_i^t) = r_i^t(s_i^t, a_i^t) + \gamma \Phi(s^{t+1}) - \Phi(s^t)$ 
10:   $Q_i(s^t, a_i^t) \leftarrow Q_i(s^t, a_i^t) + \alpha \left( r'_i + \gamma \max_{a'_i} Q_i(s^{t+1}, a'_i) - Q_i(s^t, a_i^t) \right)$ 
11: end for

```

Algorithm 2 Centralized Q-Learning with Potential Based Reward Shaping (Albrecht et al., 2024)

```

1: Initialize:  $Q(s, a) \leftarrow 0$  for all  $s \in S, a \in A = A_1 \times \dots \times A_n$ 
2: Repeat for every episode:
3: for  $t = 0, 1, 2, \dots$  do
4:   Observe current state  $s^t$ 
5:   With probability  $\epsilon$ , choose random joint action  $a^t \in A$ 
6:   Otherwise, choose joint action  $a^t \in \arg \max_a Q(s^t, a)$ 
7:   Apply joint action  $a^t$ , observe rewards  $r_1^t, \dots, r_n^t$  and next state  $s^{t+1}$ 
8:   Transform  $r_1^t, \dots, r_n^t$  into scalar reward  $r^t$ 
9:    $r' = r^t + \gamma \Phi(s^{t+1}) - \Phi(s^t)$ 
10:   $Q(s^t, a^t) \leftarrow Q(s^t, a^t) + \alpha \left( r' + \gamma \max_{a'} Q(s^{t+1}, a') - Q(s^t, a^t) \right)$ 
11: end for

```
